2004 International Symposium on Nonlinear
Theory and its Applications (NOLTA2004)
Fukuoka, Japan, Nov. 29 - Dec. 3, 2004

The buck converter planar piecewise isometry

Jonathan H.B. Deane

Department of Mathematics and Statistics,
University of Surrey,
Guildford, GU2 7XH, UK
Email: j.deane@eim.surrey.ac.uk

Abstract—We derive the mapping that describes the behaviour of a buck converter with a particular control system, and show that, in the case of zero dissipation, this map is a planar piecewise isometry, known as the Goetz map. Adding dissipation modifies the map to a 'piecewise similarity', and some properties of this map are investigated.

1. Introduction

A planar piecewise isometry (PWI) is an apparently very simple two-dimensional mapping in which the phase plane is cut into a number of disjoint subsets and each of these is rigidly rotated and shifted. Such mappings have been studied by mathematicians for a number of years, and the behaviour they exhibit is intricate and fascinating. Perhaps surprisingly, given their simple structure, mappings of this type also arise as descriptions of real electronic systems — to date, at least two such applications have been discussed in the literature, being overflow oscillations in digital filters [1] and the Σ-Δ modulator [2]– [4].

In this paper we demonstrate that a third practical electronic system, the buck converter, can be modelled in this way. We discuss the implications of adding dissipation.

2. A mapping that describes the buck converter

The buck converter, shown in figure 1, is a circuit well known amongst power electronics engineers. Its purpose is to deliver power at nominally constant voltage V_0 to a load, here represented by a resistor R in parallel with a current source I_0, from a voltage source V_i, where $V_0 \leq V_i$, and to do this efficiently.

This system is two-dimensional, the state variables being $i = i(t)$ and $v = v(t)$, the inductor (L) current and capacitor (C) voltage respectively.

2.1. Derivation of the mapping

In the circuit diagram in figure 1, all components are considered ideal, except that we allow the inductor L to have a parasitic resistance r_L. The switches S_1 and S_2 (traditionally a diode) can be in one of two discrete states, 'closed' or 'open' and they operate in anti-phase — so if S_1 is closed, S_2 is open and *vice versa*. The state of S_1, and hence S_2, is set by the control system, to be described later. It takes as inputs the state variables v and i.

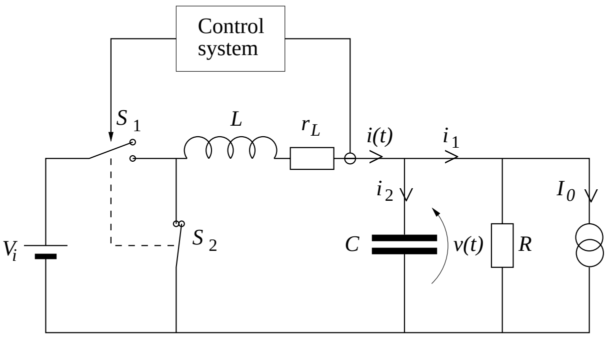

Figure 1: The circuit of the buck converter considered in this paper.

Standard circuit theory can be used to write down the following pair of differential equations to describe the buck converter:

$$L\frac{\mathrm{d}i}{\mathrm{d}t} + ir_L + v = \delta_{co}V_i, \quad i = C\frac{\mathrm{d}v}{\mathrm{d}t} + \frac{v}{R} + I_0 \tag{2.1}$$

where $\delta_{co} = 1$ when S_1 is closed and is zero when it is open. Eliminating i gives

$$a_2\frac{\mathrm{d}^2v}{\mathrm{d}t^2} + a_1\frac{\mathrm{d}v}{\mathrm{d}t} + a_0v = \delta_{co}V_i - r_LI_0 \tag{2.2}$$

where $a_2 = LC$, $a_1 = Cr_L + L/R$ and $a_0 = 1 + r_L/R$. Solving this for v gives

$$v(t) = e^{-kt}(A\cos\omega t + B\sin\omega t) + \frac{\delta_{co}V_i - r_LI_0}{a_0} \tag{2.3}$$

where A and B are arbitrary constants, $k = a_1/2a_2$, and $\omega^2 = (4a_0a_2 - a_1^2)/4a_2^2$. In practice the circuit elements would always be chosen so that ω is real. Using (2.3) in the second of equations (2.1), we find that

$$i(t)X_c = e^{-kt}\left[A(\beta\cos\omega t - \sin\omega t) + B(\beta\sin\omega t + \cos\omega t)\right] + X_c\frac{\delta_{co}V_i + I_0R}{a_0R} \tag{2.4}$$

where $X_c = 1/(\omega C)$ and $\beta = X_c(1 - kRC)/R$.

We now describe a class of control systems which set the state of the switches according to the state variables and t. Time explicitly enters the control scheme through a clock that generates a pulse every τ seconds. Some feasible control schemes are:

- (Voltage mode control) Change the state of S_1 (and hence S_2) only on the arrival of a clock pulse, and then only if v has crossed a fixed voltage threshold since the arrival of the last clock pulse.

- (Current mode control) As above, but monitor i instead of v.

- (Mixed mode control) A combination of the above, in which the switch states are inverted on the first clock pulse after the expression $iX_c \cot\phi + v_0$ has changed sign, for given constants ϕ and v_0.

For generality, we consider here the third possibility. The discontinuity is the line D in the phase plane, which has equation $v = (iX_c)\cot\phi + v_0$ — see figure 2.

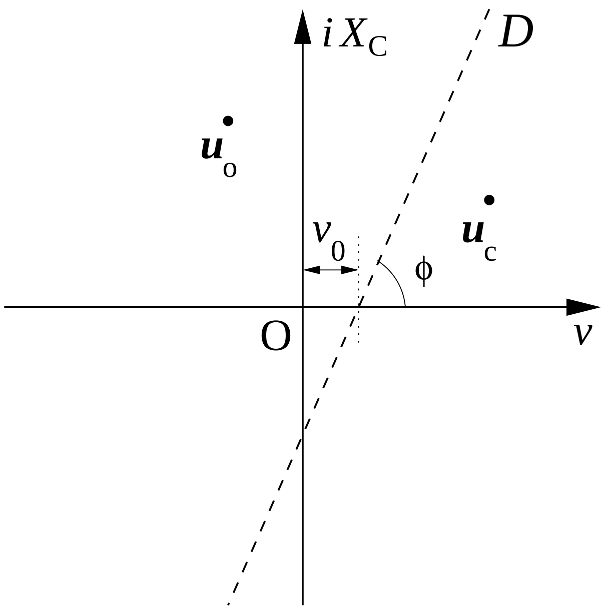

Figure 2: The control system used to set the switch states. The system evolves according to equation (2.5) with $\boldsymbol{u} = \boldsymbol{u}_o$ when $\boldsymbol{w} = [v, iX_c]^T$ lies on one side of D (dotted line), and with $\boldsymbol{u} = \boldsymbol{u}_c$ when $\boldsymbol{w}$ is on the other side of D.

Now define the state vector $\boldsymbol{w}(t) = [v(t), i(t)X_c]^T$; then using (2.3) and (2.4) at discrete times $t = n\tau$, we have

$$\boldsymbol{w}_n = \boldsymbol{w}(n\tau) = e^{-kn\tau} S(n\theta) \begin{pmatrix} A \\ B \end{pmatrix} + \boldsymbol{u} \qquad (2.5)$$

where $S(n\theta) = \begin{pmatrix} \cos n\theta & \sin n\theta \\ -\sin n\theta + \beta\cos n\theta & \cos n\theta + \beta \sin n\theta \end{pmatrix}$

with $\theta = \omega\tau$, and

$$\boldsymbol{u} = \begin{cases} \boldsymbol{u}_o = & \dfrac{I_0}{a_0}\begin{pmatrix} -r_L \\ X_c \end{pmatrix} \\ \\ \boldsymbol{u}_c = & \dfrac{I_0}{a_0}\begin{pmatrix} -r_L \\ X_c \end{pmatrix} + \dfrac{V_i}{a_0}\begin{pmatrix} 1 \\ X_c/R \end{pmatrix} \end{cases}$$

where $\boldsymbol{u}_o/\boldsymbol{u}_c$ correspond to S_1 open/closed respectively. Using equation (2.5) twice, with n and $n+1$, and eliminating $(A, B)^T$, we have, in recursive form,

$$\boldsymbol{w}_{n+1} = e^{-k\tau} S[(n+1)\theta]\, S^{-1}(n\theta)\, (\boldsymbol{w}_n - \boldsymbol{u}) + \boldsymbol{u} \qquad (2.6)$$

It is clear that D cuts $\mathbb{R}^2$ into two half-planes. We assume that ϕ and v_0 are such that $\boldsymbol{u}_o$ and $\boldsymbol{u}_c$ are in different half-planes. There are then two choices for the mapping, which we name cases S (same) and O (opposite). In case S, $\boldsymbol{u}$ in equation (2.6) is $\boldsymbol{u}_o$ (resp. $\boldsymbol{u}_c$) if $\boldsymbol{w}_n$ is in the same half-plane as $\boldsymbol{u}_o$ (resp. $\boldsymbol{u}_c$). In case O, $\boldsymbol{u}$ is $\boldsymbol{u}_o$ (resp. $\boldsymbol{u}_c$) if $\boldsymbol{w}_n$ is in the opposite half-plane to $\boldsymbol{u}_o$ (resp. $\boldsymbol{u}_c$).

2.2. Transformation into standard form

By a sequence of linear transformations Λ_a, Λ_b and Λ_c we now put equation (2.6) into standard form and reduce the number of parameters from eight (four parameters to define $\boldsymbol{u}_o, \boldsymbol{u}_c$, two to define D, θ and $e^{-k\tau}$) to four. Transformation Λ_a is defined by

$$\boldsymbol{x}_b = \Lambda_a \boldsymbol{x}_a = \begin{pmatrix} 1 & 0 \\ -\beta & 1 \end{pmatrix} \boldsymbol{x}_a$$

where $\boldsymbol{x}_a = (x_a, y_a)^T$ and $\boldsymbol{x}_b = (x_b, y_b)^T$. It is then easy to show that $\Lambda_a S(n\theta) = R(n\theta)$, the clockwise rotation matrix by an angle $n\theta$. As a side effect, Λ_a transforms D into D', which is $x_b = y_b \cot\phi' + v'_0$ where $\cot\phi' = \cos\phi/(\sin\phi - \beta\cos\phi)$ and $v'_0 = v_0 \sin\phi/(\sin\phi - \beta\cos\phi)$.
Transformation Λ_b is defined by

$$\boldsymbol{x}_c = (x_c, y_c)^T = \Lambda_b(\boldsymbol{x}_b) = \begin{pmatrix} \sin\phi' & -\cos\phi' \\ \cos\phi' & \sin\phi' \end{pmatrix} \begin{pmatrix} x_b - v'_0 \\ y_b \end{pmatrix}$$

Under this transformation, D' becomes D'' which lies along the y_c-axis. The final transformation, Λ_c, consists of a shift in the y_c-direction and a rescaling so that $\boldsymbol{u}_o$ becomes the point $(-1, 0)$. Let $\Lambda_b(\Lambda_a \boldsymbol{u}_o) = [u''_x, u''_y]^T$; then

$$\boldsymbol{x} = \Lambda_c(\boldsymbol{x}_c) = -\frac{1}{u''_x}\begin{pmatrix} x_c \\ y_c - u''_y \end{pmatrix}$$

Define $\boldsymbol{c}_0 = \Lambda_c(\Lambda_b(\Lambda_a \boldsymbol{u}_o))$, $\boldsymbol{c}_1 = \Lambda_c(\Lambda_b(\Lambda_a \boldsymbol{u}_c))$ so $\boldsymbol{c}_0$ is $(-1, 0)$; $\lambda = e^{-k\tau}$, $\boldsymbol{x}_n = \boldsymbol{x}(n\tau) = (x_n, y_n)^T = \Lambda_c(\Lambda_b(\Lambda_a \boldsymbol{w}_n))$; then the transformed version of equation (2.6) becomes $\boldsymbol{x}_{n+1} - \boldsymbol{c} = \lambda R(\theta)(\boldsymbol{x}_n - \boldsymbol{c})$ and hence

$$\boldsymbol{x}_{n+1} = \lambda R(\theta)(\boldsymbol{x}_n - \boldsymbol{c}) + \boldsymbol{c}$$

where c is c_0 or c_1. In what follows, it will be more convenient to write $z \in \mathbb{C}$ for $\boldsymbol{x}$, and so the mapping becomes

$$z_{n+1} = T(z_n) = \lambda \mathrm{e}^{-\mathrm{i}\theta}(z_n - c) + c \qquad (2.7)$$

where

$$\textbf{Case S:} \qquad c = \begin{cases} c_0 & \mathrm{Re}\, z_n < 0 \\ c_1 & \mathrm{Re}\, z_n > 0 \end{cases}$$

$$\textbf{Case O:} \qquad c = \begin{cases} c_0 & \mathrm{Re}\, z_n > 0 \\ c_1 & \mathrm{Re}\, z_n < 0 \end{cases}$$

with $\lambda, \theta \in \mathbb{R}$ and $c \in \mathbb{C}$.
We assume from now on that θ/π is irrational, the only realistic possibility since it is the product of a clock period (τ) and a combination of circuit parameters (ω). Since $k \geq 0$ and $\tau > 0$, $e^{-k\tau} = \lambda \in (0, 1]$. If $\lambda = 1$, which corresponds to no dissipation ($r_L = 0$, $R \to \infty$) then the mapping T in equation (2.7) is the Goetz map [5]–[7], a much studied member of the class of maps known as piecewise isometries. For the Goetz map, it is known that

In case S:

- A global attractor exists, known as the 8-attractor, if c_0, c_1 are co-linear, *i.e.* if $\mathrm{Im}\, c_1 = 0$. The 8-attractor consists of two discs, centred on c_0 and c_1 and tangent to the $\mathrm{Im}\, z$-axis.
- If c_0, c_1 are not co-linear and $\mathrm{Im}(c_1 - c_0)$ is small, the attractor now consists of the original 8-attractor surrounded by a number of small 'satellite' discs. A period-n orbit will visit each of these discs in turn. Java applets showing this can be found at `math.sfsu.edu/goetz/Research/Att.html`.
- If $\mathrm{Im}\, c_1$ is large enough, all orbits starting outside the 8-attractor diverge to infinity at an asymptotically linear rate.

In case O:

- A global repellor exists; that is, all initial points eventually go to infinity.

The importance of understanding the dynamics for $\lambda = 1$ in case S becomes clear in the light of the following theorem.

Theorem 1 *Let $\varepsilon = 1 - \lambda > 0$. If, in the case $\varepsilon = 0$, the mapping T exhibits a period-n coding consisting of discs of non-zero radius, and $\theta \neq 2k\pi/n$, $k \in \mathbb{Z}$, then this solution persists for sufficiently small positive ε. The discs in the $\varepsilon = 0$ case become period-n fixed points when $\varepsilon > 0$.*

This is easily proved by showing that locations of points on a given periodic orbit vary smoothly with ε.
The case $\lambda = 1$ in itself is impractical however: dissipation is a requirement in any realistic model of a buck converter. Moreover, in case S two fixed points exist, c_0 and c_1, and for $\lambda \in (0, 1)$ they are attracting. A buck converter would never be designed like this, since attraction to a fixed point would mean that the switches remained in the same state for ever, giving an output voltage tending to either 0 or V_i. Hence, of more practical interest is case O and $\lambda \in (0, 1)$, which we now discuss.

3. Dynamics — case O

In case O, we have $c_0 = -1$ and

$$T(z) = \begin{cases} T_0(z) = \lambda e^{-i\theta}(z - c_1) + c_1 & \mathrm{Re}\, z < 0 \\ T_1(z) = \lambda e^{-i\theta}(z - c_0) + c_0 & \mathrm{Re}\, z > 0 \end{cases} \qquad (3.8)$$

By contrast with case S, there are no period-1 fixed points z such that $T(z) = z$. It is possible to show that T possesses a global attractor when $\lambda \in (0, 1)$, but we can go further than this.

3.1. Bound on the attractors

We can in fact construct a closed disc $\mathcal{D}_0 \in \mathbb{C}$, centre the origin, such that T is strictly contracting for all $z \in \mathbb{C} \setminus \mathcal{D}_0$.

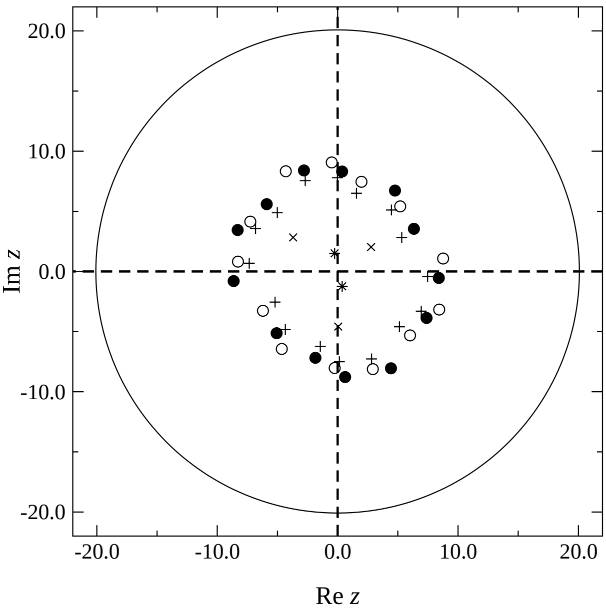

Figure 3: Illustration of Theorem 2; $\theta = 4.444341$, $c_1 = 1.12824 + 0.27769i$, $\lambda = 0.911982$. Five periodic solutions co-exist: two of period-13 with codings (1001 0011 0110 1) and (1001 0010 0110 1), black and white circles resp.; one period-16 (1011 0110 0100 1001), + sign; one of period 3 (110), $\times$; and one of period 2 (01), $*$. The circle is the boundary of $\mathcal{D}_0$ defined in Theorem 2.

Theorem 2 *Disc $\mathcal{D}_0$, defined above, is $\{z \in \mathbb{C} : |z| \leq \rho\}$ where*

$$\rho = \frac{r_{max}}{1 - \lambda} \sqrt{1 - 2\lambda \cos\theta + \lambda^2}$$

with $r_{max} = \max(|c_0|, |c_1|)$.

Proof is by direct calculation. First define $\mathcal{D}$ as the closed disc $|z| \leq r$ whose boundary, C, is the circle $|z| = r$. We first approximate $T(\mathcal{D})$ by $\tilde{T}(\mathcal{D}) = T_0(\mathcal{D}) \cup T_1(\mathcal{D})$. Since the T_j are (continuous) isometries scaled by λ, it follows that $T_j(\mathcal{D})$, $j = 0, 1$, will also be discs but with radius λr. Furthermore, points in the interior of $\mathcal{D}$ will be mapped into points inside $T_j(\mathcal{D})$. Thus $T(\mathcal{D}) \subset \tilde{T}(\mathcal{D})$, the former consisting of two half-discs rather than the two whole discs which comprise the latter. Considering now the circle $C = \partial\mathcal{D}$, substitute $z = re^{\mathrm{i}t}$ into equation (3.8) to give $T_j(C) = z_j(t)$ where

$$z_j(t) = \lambda e^{-\mathrm{i}\theta}\left(re^{\mathrm{i}t} - c_j\right) + c_j$$

with $j = 0, 1$. According to the foregoing, these expressions represent the circles $|z_j - d_j| = \lambda r$ with centres d_j, in parametric form with parameter t. Solving for d_j such that $|z_j - d_j|$ has no t-dependence gives

$$d_j = c_j\left(1 - \lambda e^{-\mathrm{i}\theta}\right).$$

To find the minimal radius ρ such that $\tilde{T}(\mathcal{D}) \subset \mathcal{D}$ we observe that $\rho = |d_j| + \lambda\rho$ so that $\rho = |d_j|/(1 - \lambda)$. From the definition of d_j and the condition of minimality, the result follows. □

Hence, all periodic solutions must lie within the disc $\mathcal{D}_0$. That this bound can be quite good is illustrated in figure 3. The coding referred to in the caption there is the sequence in which points on a given orbit visit the half planes, with $0 : \mathrm{Re}\, z < 0,\ 1 : \mathrm{Re}\, z > 0$.

3.2. Dynamics — numerical results

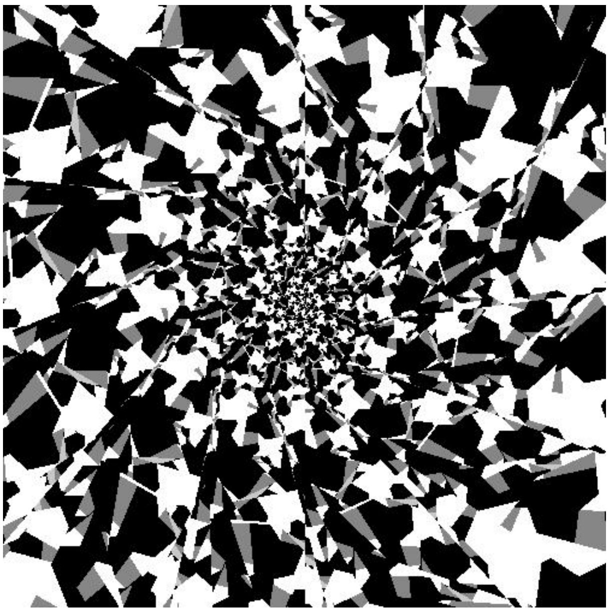

Figure 4: Basins of attraction for co-existing period-6 (black), period-3 (white), period-7 (dark grey) and period-6 (light grey) solutions when $\theta = 5.80218384$, $c_1 = 0.371745 + 0.370210\mathrm{i}$, $\lambda = 0.912810$.

Extensive computer searches for solutions to equation (2.7) have been carried out, and only periodic solutions have ever been found. The periods of the solutions vary widely and many different solutions can co-exist — it is not unusual to observe seven or more co-existent solutions. The basins of attraction in a case in which four periodic solutions co-exist are shown in figure 4. A proof of the non-existence of any other type of solution to this equation, for example chaotic or quasi-periodic ones, is presently lacking.

The conjectured non-chaotic nature of solutions contrasts with earlier work of the author [8] where chaotic behaviour in the buck converter was observed both experimentally and numerically. That result is not at variance with the present work however, as a different control system, pulse width modulation by natural sampling, was used there. Additionally, the mapping in that case cannot be written in closed form — and not as a piecewise similarity.

Basins of attraction for the periodic solutions have also been approximated numerically. These can be intricate and it is interesting to note that some solutions appear to have a finite basin of attraction whereas others are infinite.

Acknowledgements

The author would like to thank Arek Goetz and Peter Ashwin for profitable and stimulating discussions.

References

[1] M.J. Ogorzałek, Complex behaviour in digital filters, *Int. J. of Bifurcation and Chaos*, 2(1), pp. 11–29 (1992)

[2] O. Feely and D. Fitzgerald, Non-ideal and chaotic behaviour in bandpass sigma-delta modulators, *Proceedings of NDES 1996*, Sevilla, Spain, pp. 399–404 (1996)

[3] P.Ashwin, J.H.B. Deane and X-C. Fu, Dynamics of a bandpass sigma-delta modulator as a piecewise isometry, *Proceedings, ISCAS 2001*, pp III-811 – III-814 (Sydney, Australia, 2001)

[4] O. Feely *et al.*, Nonlinear dynamics of bandpass sigma-delta modulation, *Int. J. of Bifurcation and Chaos*, 10(2), pp. 303–327 (2000)

[5] A. Goetz, Perturbations of 8-attractors and births of satellite systems, *Int. J. of Bifurcation and Chaos*, 8(10), 1937–1956 (1998)

[6] A. Goetz, Dynamics of piecewise isometries, *Illinois Journal of Mathematics*, 44(3), pp. 465–478 (2000)

[7] A. Goetz, A self-similar example of a piecewise isometric attractor, *Dynamical systems (Luminy-Marseille)*, World Scientific Publishing, River Edge NJ, pp. 248–258 (1998)

[8] J.H.B. Deane and D.C. Hamill, Analysis, simulation and experimental study of chaos in the buck converter, *Power Electronics Specialists Conference Record*, vol. II, pp. 491–498 (1990)